Experimental and theoretical studies of reactions of neutral vanadium and tantalum oxide clusters with NO and NH_3

S. Heinbuch, F. Dong, J. J. Rocca, and E. R. Bernstein'

Experimental and theoretical studies of reactions of neutral vanadium and tantalum oxide clusters with NO and NH₃
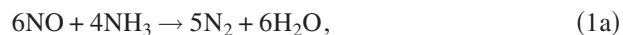
S. Heinbuch,[2,3] F. Dong,[1,2] J. J. Rocca,[2,3] and E. R. Bernstein[1,2,a]

[1]*Department of Chemistry, Colorado State University, Fort Collins, Colorado 80523, USA*
[2]*NSF ERC for Extreme Ultraviolet Science and Technology, Colorado State University, Fort Collins, Colorado 80523, USA*
[3]*Department of Electrical and Computer Engineering, Colorado State University, Fort Collins, Colorado 80523, USA*

Reactions of neutral vanadium and tantalum oxide clusters with NO, NH₃, and an NO/NH₃ mixture in a fast flow reactor are investigated by time of flight mass spectrometry and density functional theory (DFT) calculations. Single photon ionization through a 46.9 nm (26.5 eV) extreme ultraviolet (EUV) laser is employed to detect both neutral cluster distributions and reaction products. Association products VO₃NO and V₂O₅NO are detected for V_mO_n clusters reacting with pure NO, and reaction products, $TaO_{3,4}(NO)_{1,2}$, Ta_2O_5NO, $Ta_2O_6(NO)_{1-3}$, and $Ta_3O_8(NO)_{1,2}$ are generated for Ta_mO_n clusters reacting with NO. In both instances, oxygen-rich clusters are the active metal oxide species for the reaction $M_mO_n + NO \rightarrow M_mO_n(NO)_x$. Both V_mO_n and Ta_mO_n cluster systems are very active with NH₃. The main products of the reactions with NH₃ result from the adsorption of one or two NH₃ molecules on the respective clusters. A gas mixture of NO:NH₃ (9:1) is also added into the fast flow reactor: the V_mO_n cluster system forms stable, observable clusters with only NH₃ and no $V_mO_n(NO)_x(NH_3)_y$ species are detected; the Ta_mO_n cluster system forms stable, observable mixed clusters, $Ta_mO_n(NO)_x(NH_3)_y$, as well as $Ta_mO_n(NO)_x$ and $Ta_mO_n(NH_3)_y$ individual clusters, under similar conditions. The mechanisms for the reactions of neutral V_mO_n and Ta_mO_n clusters with NO/NH₃ are explored via DFT calculations. Ta_mO_n clusters form stable complexes based on the coadsorption of NO and NH₃. V_mO_n clusters form weakly bound complexes following the reaction pathway toward end products N₂ + H₂O without barrier. The calculations give an interpretation of the experimental data that is consistent with the condensed phase reactivity of V_mO_n catalyst and suggest the formation of intermediates in the catalytic chemistry. © *2010 American Institute of Physics.* [doi:10.1063/1.3497652]

I. INTRODUCTION

Selective catalytic reduction (SCR) of nitric oxide by ammonia over V₂O₅/TiO₂ based catalysts is the most advanced and widely used technology capable of reducing NO_x emissions to the low levels mandated in many areas of the world.[1] The overall catalytically promoted reactions are

$$6NO + 4NH_3 \rightarrow 5N_2 + 6H_2O, \tag{1a}$$

$$6NO_2 + 8NH_3 \rightarrow 7N_2 + 12H_2O, \text{ etc.} \tag{1b}$$

In the condensed phase, a vanadium oxide catalyst is loaded on an anatase support as a monolayer, and the active VO_x species is suggested to have monomeric or dimeric structures.[2] These VO_x structures are considered to be preferable as active sites rather than bulk V₂O₅. They are proposed to consist of terminal oxygen atoms that can be saturated by molecules like ammonia or water.[3–5] Catalyst development for this process aims to improve efficiency, avoid parallel reactions, and to reach lower working temperatures.

Although numerous experimental surface studies have been carried out on the NO SCR reaction over vanadium based catalysts, a complete elucidation of the reaction mechanism has not been achieved, and very few, if any, gas phase experiments have been conducted. The reaction is generally believed to occur through an Eley–Rideal type mechanism in which ammonia is adsorbed on the vanadium based catalyst in the first step, and then the reaction proceeds with the activation of nitric oxide from the gas phase;[6–23] however, the adsorption mode of ammonia on the catalytic surface is still unclear.

Using temperature programmed desorption (TPD) and IR studies, Inomata *et al.*[6,7] suggest that the active site for the ammonia activation is the Brønsted acidic V—OH site adjacent to a $V^{5+}O$ site. Because of an additional H, ammonia is suggested to be adsorbed on this site as NH_4^+. Topsøe[10–12] and Gasior *et al.*[13] both suggest that predominantly Brønsted acid sites (V—OH) are present and active on the surface of oxidized V₂O₅ for the ammonia activation reaction. Following this idea, Ozkan *et al.*[14] conclude that ammonia adsorbs on pairs of V—OH groups, leading to the formation of surface ammonium ion species. Gilardoni *et al.*[24,25] propose that after nitric oxide interaction with preadsorbed NH_4^+ species, NH_2NO species form in the gas phase, which then undergo a

a)Electronic mail: erb@lamar.colostate.edu.

series of isomerization reactions to give reaction products nitrogen and water. Similarly, Anstrom *et al.*[26,27] investigated the role of V_2O_5 in the reaction of adsorbed NH_4^+ with nitric oxide by using a vanadium oxide cluster containing four vanadium atoms with a Brønsted acidic V—OH site. According to density functional theory (DFT) calculations by Yin *et al.*[28] for the mechanism of SCR of NO by NH_3 over a V_2O_5 surface, two hydroxyl groups (V—OH) are responsible for the formation of NH_4^+ species, and a VO group is required for activation of NH_4^+. Aside from adsorption as NH_4^+, a different approach to the SCR of NO by NH_3 suggests that NH_3 adsorbs and dissociates into NH_2 and H, and that the formation of the ammonium ion is a stable intermediate.[18,29,30]

Zhanpeisov *et al.*[30] find that the NH_4^+ species is not favorable from an energetic point of view and report an energy gain of 47.7 kcal/mol for the NH_3 dissociation on a reactive O site. Janssen *et al.*,[8,9] employing isotopic transient studies, consider the VO species to be the active site that is easily reduced. According to this study, ammonia is adsorbed on this site as V—ONH_2 by reducing the adjacent VO site to V—OH. Ramis *et al.*[15–18] suggest that Brønsted acidity is not a necessary requirement for SCR activity and that ammonia is activated for SCR by coordination over Lewis acidic sites on TiO_2 as well. This activated ammonia is easily transformed to the amide NH_2 species by hydrogen abstraction. Aside from the examples given above, additional theoretical studies employing the cluster approach to vanadia/titania models have been reported.[18,31–34]

Recently, single photon ionization (SPI) through EUV laser radiation (46.9 nm) has been successfully implemented by our group to study a series of neutral metal oxide clusters and their reactions. We have shown that minor cluster fragmentation during the ionization process by a 26.5 eV laser does not affect our observation of the neutral cluster distribution.[35–45] The EUV laser is demonstrated to be essential in the detection of all neutral clusters and their products by time of flight mass spectrometry.

In the present work, a fast flow reactor is employed to study the reactivity of neutral vanadium and tantalum oxide clusters toward NO, NH_3, and an NO/NH_3 mixture. The motivation is to generate possible molecular level mechanisms for the SCR of NO by NH_3 in condensed phase catalytic reactions. In this report, the experimental results are presented and discussed based on DFT calculations. The DFT calculation results occupy a unique position in the analysis of our experimental results because, without them, one can incorrectly conclude that the lack of observed intermediate species for V_mO_n clusters reacting with NO/NH_3 compared to those formed for Ta_mO_n clusters, signals an inactivity of V_mO_n clusters to generate and model the condensed phase behavior. Based on the DFT calculations, such a conclusion is incorrect; in fact, quite the opposite is true. Additionally, these calculations demonstrate that a mechanism generating the $HOV_mO_{n-1}NH_2$ reaction intermediate is appropriate for the SCR of NO with NH_3 on a V_mO_n catalytic cluster.

II. EXPERIMENTAL PROCEDURES

The experimental apparatus has been described in detail elsewhere.[40–43] Briefly, M_mO_n (M=V or Ta) clusters are generated by laser ablation with a focused 532 nm laser ($\sim$10 mJ/cm^2) onto a translational and rotational (spiral) motion metal target in the presence of a pulsed helium carrier gas mixed with 0.5% O_2. Concentration of oxygen in the carrier gas is kept low so as not to interfere with study of the V_mO_n/Ta_mO_n+NO/NH_3 reaction in the fast flow reactor cell. Metal oxide clusters are formed in an adjustable length gas channel with a "waiting room" upstream. The gas channel is coupled directly to a tube/reactor (6.3 mm inner diameter by 76 mm length). The pure reactant gases, NO, NH_3, or NO:NH_3 mixture (9:1) are injected into the reactor by a second pulsed valve. The delay time between the two valve openings is optimized to yield the best product signals. Pressure in the fast flow reactor is estimated to be about 1 Torr in the presence of a reactant gas pulse and reaction time is about 50 μs. After the flow tube reactor, the ions created in the ablation source and flow tube reactor are removed by an electric field. Mass resolution for the time of flight mass spectrometer is good enough to resolve l amu at 1000 amu. Neutral clusters and products in the beam are ionized by a 46.9 nm capillary discharge EUV laser that is described in detail in the literature.[44,45]

The EUV laser pulse energy is $\sim$10 μJ at the output of the laser, but is reduced to $\sim$3–5 μJ at the output of a z-fold mirror system placed just before the ionization region with the purpose of providing alignment capability of the laser beam with respect to the cluster beam. The EUV laser is not tightly focused in the ionization region to avoid multiphoton ionization and a Coulomb space charge effect due to He$^+$ ions produced by 26.5 eV ionization of He in the molecular beam. A mass gate is set before the microchannel plate (MCP) in order to gate large He signals and prevent saturation of the detector.

The EUV laser is especially important for the study of metal oxide clusters because it ionizes all the neutral clusters and their neutral reaction products by single photon transitions. Issues dealing with back flow gas from the reaction flow tube, ions present in the beam that interfere with neutral cluster chemistry, and ionization by EUV laser photons are discussed in previous publications.[35–43] Decaying tails observed at later signal times in the mass spectra are caused by spontaneous emission from the Ar plasma generated with the EUV laser radiation with a decay time of 100 ns. The laser pulse width is about 1.5 ns.

III. COMPUTATIONAL DETAILS

DFT calculations using the GAUSSIAN 03 program[46] are employed to study reactions of neutral V_mO_n and Ta_mO_n clusters with NO, NH_3, and NO/NH_3. The DFT calculations involve geometry optimization of various reaction intermediates and transition states. Transition state optimizations are performed by using the synchronous transit-guided quasi-Newton method.[47,48] Vibrational frequencies are calculated to check that the reaction intermediates have all positive frequencies and species in the transition states have only one

TABLE I. Comparison of calculated and experimental bond energies (D_{298k}) and bond lengths for V_mO_n and Ta_mO_n clusters and reaction partners NO and NH_3.

	Experiment	B3LYP/TZVP	B3LYP/LANL2TZ
	D_{298k} (eV), bond length (Å)	D_{298k} (eV), bond length (Å)	D_{298k} (eV), bond length (Å)
NO	6.5[a]	6.4	
	1.150[a]	1.147	
NH_3	3.99 ± 0.22[b]	4.01	
	1.012[a]	1.013	
^{4}VO	6.44 ± 0.2,[c] 6.48 ± 0.1[d]		6.16
	1.589[e]		1.583
^{2}TaO	8.29 ± 0.23,[c] 8.16 ± 0.12[f]		7.79
	1.687[a]		1.687

[a]Reference 54(a). [d]Reference 54(d).
[b]Reference 54(b). [e]Reference 54(a).
[c]Reference 54(c). [f]Reference 54(e).

imaginary frequency. Intrinsic reaction coordinate (IRC) calculations[49] are also performed so that a transition state connects two appropriate local minima in the reaction paths. The hybrid B3LYP exchange-correlation functional[50] is adopted. A contracted Gaussian basis set of triple zeta valence (TZVP) quality[51] for H, N, and O atoms is used and the LANL2TZ (Ref. 52) basis set with the corresponding effective core potentials is used for all metal atoms. Test calculations indicate that basis set superposition error (BSSE) (Ref. 53) corrections are negligible (~1–2 kcal/mol), so the BSSE correction is not taken into consideration in this study. The comparison of calculated results with experimental data is listed in Table I. B3LYP/LANL2TZ theory method and basis set is good enough to calculate V_mO_n and Ta_mO_n clusters and their reactions with NO and NH_3.

Wave function spin contamination is not a serious problem for these cases (VO_3, TaO_3, V_2O_5NO, and Ta_2O_5NO) at the B3LYP theory level because $\langle S^2 \rangle$ values are uniform and deviate only slightly from the pure spin values 0.75. The spin states marked on the calculated structures are the lowest energy states for the structures.

IV. RESULTS AND DISCUSSION

To study reactions of neutral M_mO_n (M=V or Ta) clusters with NO, NH_3, or NO/NH_3 (9:1), mixed reactant/He gas is pulsed into the reactor at a pressure of ~15 psi. When the neutral metal oxide clusters generated from the ablation/expansion source pass through the fast flow reactor cell, collisions occur between neutral M_mO_n clusters and reactant molecules. The instantaneous reactant gas pressure in the reactor cell (during the time that M_mO_n is in the cell) is estimated to be about 1 Torr. New reaction products and the remnant neutral M_mO_n clusters are detected by 26.5 eV, EUV laser single photon ionization as shown in Figs. 1 and 2. Observed products in the reaction of V_mO_n and Ta_mO_n with NO, NH_3, and mixed NO/NH_3 reactants are listed in Table II.

The high photon energy of 26.5 eV radiation might possibly fragment/photodissociate neutral clusters or their reaction products during the ionization process, and thereby confuse the identification of ground state neutral species

chemistry. In order to clarify this issue, a comparison experiment is conducted in which both 10.5 and 26.5 eV lasers are used for ionization in the study of V_mO_n cluster reactions with NO and NH_3. Near threshold, single photon ionization using a 10.5 eV laser photon cannot leave enough excess energy in the clusters to fragment any vanadium oxide cluster or break any chemical bond of the reaction products following ionization of the neutral species.[35–43] Comparing the
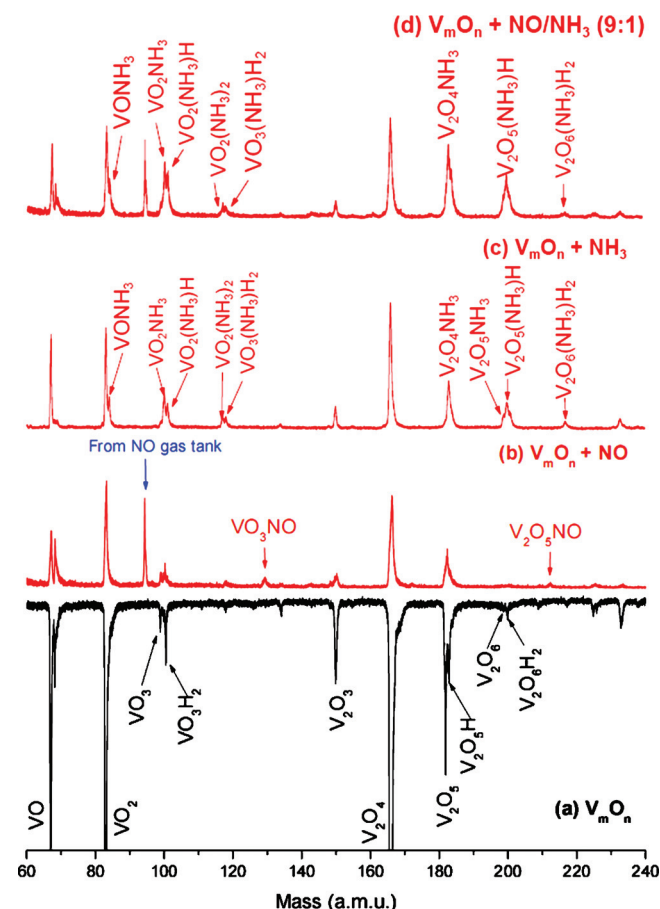

FIG. 1. Mass spectra of reactions of V_mO_n clusters with NO, NH_3, and NO:NH_3 (9:1) ionized by a 26.5 eV EUV laser. The reactant gases (800 Torr) are added to the flow tube reactor. Very few new products of the reactions are detected.
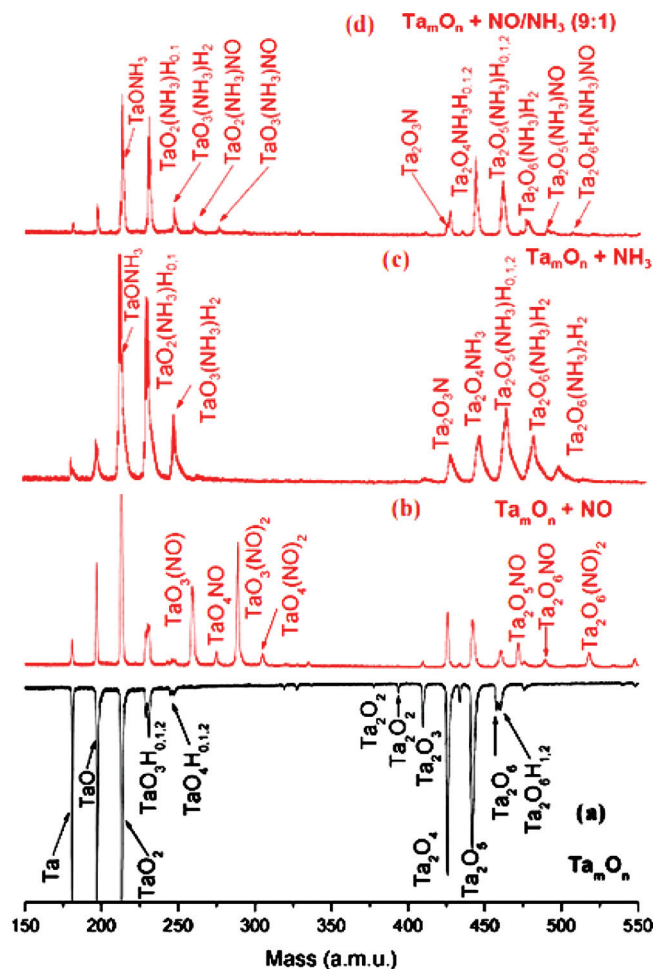
FIG. 2. Mass spectra of reactions of Ta_mO_n clusters with NO, NH_3, and NO:NH_3 (9:1) ionized by a 26.5 eV EUV laser. The reactant gases (800 Torr) are added to the flow tube reactor. Many new products of the reactions are detected.

resulting spectra from both ionization methods, we find that the reaction products present are almost the same. Our conclusion is that the fragmentation or photodissociation of neutral vanadium oxide clusters and their reaction products caused by a single 26.5 eV photon can be neglected in these experiments, as well documented in Ref. 43 for V_mO_n, Nb_mO_n, and Ta_mO_n samples at both 26.5 and 10.5 eV ionization energies. In our previous work, we have found that the distribution of neutral V_mO_n clusters is nearly the same using either method for ionization, except that some oxygen-rich clusters with high ionization energies ($>$10.5 eV) cannot be detected by 10.5 eV single photon ionization.[43] The reason we prefer to use the 26.5 eV laser as the ionization source is that it can ionize all the neutral metal oxide clusters generated in the expansion/ablation source and all reaction products generated in the reactor.

Figures 1(a) and 2(a) show neutral V_mO_n and Ta_mO_n cluster distributions in a certain mass region without reaction gas in the fast flow reactor. A similar cluster distribution is observed for neutral V_mO_n and Ta_mO_n clusters except more oxygen-rich clusters are generated for Ta_mO_n. Three kinds of vanadium oxide clusters are identified: (1) the most stable stoichiometric structures VO_2, V_2O_4/V_2O_5, V_3O_7, V_4O_{10}, V_5O_{12}, etc., as demonstrated experimentally and

theoretically,[43,55,56] (2) oxygen deficient vanadium oxide clusters VO, $V_2O_{2,3}$, $V_3O_{5,6}$, $V_4O_{8,9}$, $V_5O_{9,10,11}$, and $V_6O_{13,14}$, they are missing one or two oxygen atoms compared to the most stable clusters and present a tendency to become the most stable clusters by reacting with O or O_2,[56] and (3) a few oxygen-rich clusters, VO_3, V_3O_8, and V_5O_{13}, etc., they have one or more oxygen atoms compared to the most stable clusters and present a tendency to lose O or O_2 and become the most stable clusters.[56] Additionally, one can find that the latter oxygen-rich neutral vanadium oxide clusters are almost always present with one or more attached hydrogen atoms, such as VO_3H_2, $V_2O_6H_2$, $V_3O_8H_{1,2}$, etc.[43] The stability of V/O and V/O/H cluster ions are studied by Schwartz *et al.*[57(a)] and Castleman *et al.*[57(b)]

Decay fractions $(I_0-I)/I_0$ of the V_mO_n signals in the reactions with NH_3 can obtained from Figs. 1 and 2, in which I_0 and I are the intensities of V_mO_n signal before and after reaction with NH_3, respectively. The decrease of the signals caused by collisions with He and reactant NH_3 is estimated based on the signal changes of V_2O_3, V_3O_5 clusters, etc. (see Fig. 1), which have almost no reactions with NH_3 molecules. Under our experimental conditions (estimated NH_3 partial gas pressure 1 Torr and reaction time $\sim$50 μs), the pseudo-first-order rate constants k [$\ln(I/I_0)=-Ckt$], in which C is the concentration of reactant in the reactor, are calculated as 0.6 (VO), 1.1 (VO_2), and 2.4 (V_2O_4), $\times 10^{-13}$ cm^3 s^{-1}.

Three kinds of Ta_mO_n clusters are also observed: (1) the most stable stoichiometric clusters, TaO_2, Ta_2O_4/Ta_2O_5, Ta_3O_7, etc., (2) oxygen deficient tantalum oxide clusters, TaO, $Ta_2O_{2,3}$, and $Ta_3O_{5,6}$, and (3) oxygen-rich clusters, $TaO_{3,4}$, Ta_2O_6, and Ta_3O_8. In the mass spectrum, oxygen-rich, neutral tantalum oxide clusters are almost always present with one or more attached hydrogen atoms, such as TaO_4H, $Ta_2O_6H_2$, etc.[43] Oxygen-rich Ta_mO_n clusters appear relatively more abundant than do oxygen-rich V_mO_n clusters in their respective neutral cluster distributions. In Fig. 2, one finds that the signal intensities of products TaO_3(NO) and TaO_3(NO)$_2$ [Fig. 2(b)] are much stronger than the TaO_3 reactant intensity [Fig. 2(a)]; this behavior may be due to an ionization cross section change from Ta_mO_n to Ta_mO_n(NO)$_x$.

A. Structure and reaction mechanism for neutral M_mO_n+NO

1. Experimental results

Two association products, VO_3NO and V_2O_5NO, for the reactions V_mO_n+NO, are observed in Fig. 1(b) when NO is added to the fast flow reactor. They are generated from association reactions,

$$M_mO_n + NO \rightarrow M_mO_nNO, \tag{2}$$

and stabilized (cooled) by third body (usually He) collisions. Note that no oxygen deficient clusters are involved in the association products. The peak present at mass 94 is found to be a contaminant from the NO gas tank. In addition, no reaction product is observed when NO_2 gas is added to the reactor cell. If pure He gas is added to the reactor cell all

TABLE II. Observed V$_m$O$_n$ and Ta$_m$O$_n$ clusters and their reaction products with NO, NH$_3$, and mixed NO/NH$_3$ reactants. The numbers in the brackets are the calculated ΔH_{react} in eV for the reactions V$_m$O$_n$+NO$\rightarrow$V$_m$O$_n$NO or V$_m$O$_n$+NH$_3$$\rightarrow$V$_mO_nNH_3$ at 298 K.

	V$_m$O$_n$ (calculated ΔH_{react}) eV	Ta$_m$O$_n$ (calculated ΔH_{react}) eV	V$_m$O$_n$ cluster distribution (mV)	Ta$_m$O$_n$ cluster distribution (mV)
+NO	VO$_3$(NO) (-2.0)	TaO$_3$(NO) (-1.8)	VO(74)	TaO(637)
	V$_2$O$_5$(NO) (-1.3)	TaO$_3$(NO)$_2$	VO$_2$(131)	TaO$_2$(672)
		TaO$_4$(NO)	VO$_3$(8)	TaO$_3$(64)
		TaO$_4$(NO)$_2$		TaO$_4$(13)
		Ta$_2$O$_5$NO (-1.0)	V$_2$O$_3$(24)	Ta$_2$O$_3$(58)
		Ta$_2$O$_6$(NO)	V$_2$O$_4$(216)	Ta$_2$O$_4$(253)
		Ta$_2$O$_6$(NO)$_2$	V$_2$O$_5$(48)	Ta$_2$O$_5$(221)
		Ta$_3$O$_8$(NO)	V$_2$O$_6$(5)	Ta$_2$O$_6$(36)
		Ta$_3$O$_8$(NO)$_2$	V$_3$O$_6$(134)	Ta$_3$O$_6$(54)
+NH$_3$	VO(NH$_3$)	TaO(NH$_3$)	V$_3$O$_7$(221)	Ta$_3$O$_7$(205)
	VO$_2$(NH$_3$) (-2.7)	TaO$_2$(NH$_3$)	V$_3$O$_8$(30)	Ta$_3$O$_8$(30)
	VO$_2$(NH$_3$)$_2$	TaO$_2$(NH$_3$)H$_{0,1}$		
	VO$_2$(NH$_3$)H (-1.0)	TaO$_3$(NH$_3$)H$_2$		
	VO$_3$(NH$_3$)H$_2$ (-1.0)	Ta$_2$O$_4$(NH$_3$)		
	V$_2$O$_4$(NH$_3$) (-1.6)	Ta$_2$O$_5$(NH$_3$)		
	V$_2$O$_5$(NH$_3$) (-3.0)	Ta$_2$O$_5$(NH$_3$)H$_{1,2}$		
	V$_2$O$_5$(NH$_3$)H$_{1,2}$	Ta$_2$O$_6$(NH$_3$)H$_2$		
	V$_2$O$_6$(NH$_3$)H$_2$	Ta$_2$O$_6$(NH$_3$)$_2$H$_2$		
+NH$_3$+NO	No products observed	TaO$_2$(NH$_3$)(NO)		
		TaO$_3$(NH$_3$)(NO)		
		Ta$_2$O$_5$(NH$_3$)(NO)		
		Ta$_2$O$_6$H$_2$(NH$_3$)(NO)		

cluster signals decrease in roughly the same proportion due to scattering by inert gas in the reactor.

Figure 2(b) displays the mass spectrum of reactants and products for the reaction of Ta$_m$O$_n$ clusters with NO. Many association products, TaO$_3$(NO)$_{1,2}$, TaO$_4$(NO)$_{1,2}$, Ta$_2$O$_5$NO, Ta$_2$O$_6$(NO)$_{1,2,3}$, and Ta$_3$O$_8$(NO)$_{1,2}$ are observed when NO is added to the reactor. They are generated from association reactions [Eq. (2)]. Note that stable and oxygen-rich clusters both contribute to the association products. No oxygen deficient clusters are involved in the reaction. Weak signals for V$_m$O$_n$NO compared to Ta$_m$O$_n$NO, as presented in Figs. 1 and 2, can be attributed to fewer oxygen-rich V$_m$O$_n$ clusters than oxygen-rich Ta$_m$O$_n$ clusters generated under the reported experimental conditions. If NO$_2$ gas is added to the reactor cell, as many association products are observed for Ta$_m$O$_n$ reacting with NO$_2$ as are observed for Ta$_m$O$_n$ reacting with NO. The mass spectrum of Fig. 1(b) is obtained for an average of 250 laser pulses. The signal to noise ratio for the VO$_3$NO signal is larger than 4:1; significantly the reaction product VO$_3$NO is generated from the reaction of VO$_3$+NO. These results do not depend on the oxygen concentration in the expansion gas, but are a function of the chemistry difference between the V$_m$ and Ta$_m$ species in the ablation plume.

In the condensed phase, a weak interaction of NO with the V$_m$O$_n$ catalyst is supported by a number of experiments. The conventional SCR process on V$_2$O$_5$/anatase (TiO$_2$) support proceeds according to an Eley–Rideal type mechanism in which ammonia is adsorbed on the vanadium based catalyst in the first step, and the reaction then proceeds with the activation of nitric oxide from the gas phase.[6–23] One supporting argument for this type of reaction is that vanadium based catalysts do not appear as efficient as other catalysts

for NO decomposition or oxidation.[17] A different argument is supported through isotopic labeling experiments, however.[9,14] These studies suggest that the oxygen atom of the NO molecule is exchanged for an oxygen atom of a vanadyl V=O group. Through isotopic labeling experiments, one demonstrates that NO interacts actively with the V$_2$O$_5$/TiO$_2$ surface implying stronger interaction than usually postulated; however, the exchange is fast and the data suggest[9,14] that NO does not reside on the surface to react with ammonia. The SCR proceeds via NH$_3$ adsorption and interaction with a gaseous NO species.

In the present gas phase studies, only few association products (VO$_3$NO and V$_2$O$_5$NO) are generated from V$_m$O$_n$+NO reactions, while many association products are generated for Ta$_m$O$_n$+NO reactions. This seems to suggest that the interaction between V$_m$O$_n$ and NO must be weak. On other hand, condensed phase isotope exchange studies[9,14] indicate that NO and the vanadium oxide surface have a relatively strong interaction. As pointed out above, the apparent fewer interaction products for NO and V$_m$O$_n$ clusters compared to those for NO and Ta$_m$O$_n$ clusters are not necessarily due to interaction differences; it can be associated with nascent M$_m$O$_n$ cluster distribution differences. A comparison of V$_m$O$_n$ and Ta$_m$O$_n$ cluster distributions shows that oxygen-rich V$_m$O$_n$ (VO$_3$, V$_3$O$_8$, etc.) and V$_2$O$_5$ clusters are much less abundant than are oxygen-rich Ta$_m$O$_n$ (TaO$_3$, TaO$_4$, Ta$_3$O$_8$, etc.) and Ta$_2$O$_5$ clusters in the mass spectrum (Figs. 1 and 2). Note that all the reaction products are generated from oxygen-rich metal oxide clusters except for V$_2$O$_5$/Ta$_2$O$_5$. Thus, association products generated through oxygen-rich V$_m$O$_n$+NO reactions are less abundant than those for oxygen-rich Ta$_m$O$_n$+NO reactions. Theoretical results can
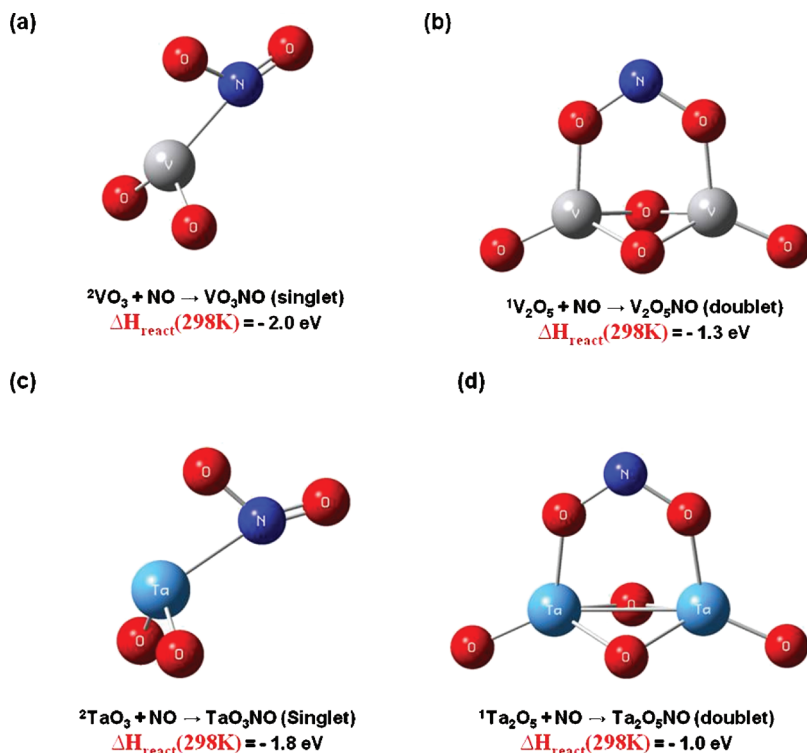
(a)

(b)

$^2VO_3 + NO \rightarrow VO_3NO$ (singlet)
$\Delta H_{react}(298K) = -2.0$ eV

$^1V_2O_5 + NO \rightarrow V_2O_5NO$ (doublet)
$\Delta H_{react}(298K) = -1.3$ eV

(c)

(d)

$^2TaO_3 + NO \rightarrow TaO_3NO$ (Singlet)
$\Delta H_{react}(298K) = -1.8$ eV

$^1Ta_2O_5 + NO \rightarrow Ta_2O_5NO$ (doublet)
$\Delta H_{react}(298K) = -1.0$ eV

FIG. 3. DFT results showing the most stable structures for reaction products (a) VO_3NO, (b) V_2O_5NO, (c) TaO_3NO, and (d) Ta_2O_5NO. $\Delta H_{react}(298 \text{ K})$ is calculated for the reaction $V_mO_n + NO \rightarrow V_mO_nNO$.

supply more information about the interaction between vanadium/tantalum oxide clusters and NO molecules as discussed in next section.

2. Theoretical results

To explore and understand the mass spectral data for V_mO_n/Ta_mO_n, clusters interacting and reacting with NO, DFT calculations are required. These calculations are undertaken with the B3LYP hybrid functional and a TZVP basis set for N and O atoms and a LANL2TZ basis set for V and Ta atoms. This level of theory is used to verify V_mO_n cluster structures calculated in Ref. 56. The comparison of calculated results with experimental data is listed in Table I. B3LYP/LANL2TZ theory method and basis set are sufficient to calculate V_mO_n and Ta_mO_n clusters and their reactions with NO and NH_3. Starting with the structures for VO_3 and V_2O_5, geometry optimizations are performed for the association products VO_3NO and V_2O_5NO, and the results are presented in Figs. 3(a) and 3(b), respectively. For VO_3NO, the most stable structure depicts that NO binds to the V atom and forms an NO_2 molecule bound to a VO_2 moiety with $\Delta H_{react}(298 \text{ K}) = -2.0$ eV [Fig. 3(a), $\Delta H_{react}(298 \text{ K})$ is calculated for the reaction $V_mO_n + NO \rightarrow V_mO_nNO$]. In the reaction, an oxygen transfers from the VO_3 molecule to the NO moiety without a barrier. The calculated V—N bond length is 2.01 Å. For V_2O_5NO, starting from an OVO_2VO_2 structure and adding NO, a bicyclic isomer [shown in Fig. 3(b)], for which the two vanadium atoms are in a distorted tetrahedral oxygen environment, is found. The calculated $\Delta H_{react}(298 \text{ K})$ for the reaction $V_2O_5 + NO \rightarrow V_2O_5NO$ is -1.3 eV, which is smaller than the -2.7 eV found by Ref.

18. This difference is due to the different computational methods employed. In our study, we use the same DFT functional (B3LYP) and basis set (LANL2TZ/TZVP) to calculate V_mO_n and Ta_mO_n clusters reacting with NO, NH_3, and NO/NH_3 in order to obtain the association energy and potential energy surface for the observed reactions.

Similar calculations are performed for the tantalum oxide cluster series in an attempt to discern the difference between NO adsorption on neutral V_mO_n and Ta_mO_n clusters. The resulting lowest energy structures for the products of tantalum oxide clusters in reaction with NO follow the results for vanadium oxide clusters with no significant differences found for the adsorption energies [Figs. 3(c) and 3(d)]. The reaction and binding between the MO_3 cluster and NO is through an O transfer from MO_3 to the NO moiety and the formation of a M–N bond: this process is also barrierless. In the case of the larger M_2O_5 cluster, NO can attach to the cluster through an O–M bond to form an M–O—N—O–M bridge. On the basis of theoretical calculations (B3LYP/LANL2TZ/TZVP), the $\Delta H_{react}(298 \text{ K})$ for $V_2O_5 + NO/VO_3 + NO$ are very close to those of $Ta_2O_5 + NO/TaO_3 + NO$. Therefore, the apparent fewer interaction products of NO and V_mO_n clusters compared to those for NO and Ta_mO_n clusters is due to the nascent cluster distribution difference for Ta_mO_n and V_mO_n (i.e., the Ta_mO_n oxygen-rich clusters are relatively more abundant than are the oxygen-rich V_mO_n clusters) and is not necessarily due to interaction or reaction differences. On the basis of our calculations, oxygen transfer from V_mO_n to the N atom of NO in the reactions of $VO_3/V_2O_5 + NO$ and $TaO_3/Ta_2O_5 + NO$ to form the lowest energy structures, as shown in Figs. 3(a) and 3(b), is a barrierless process.
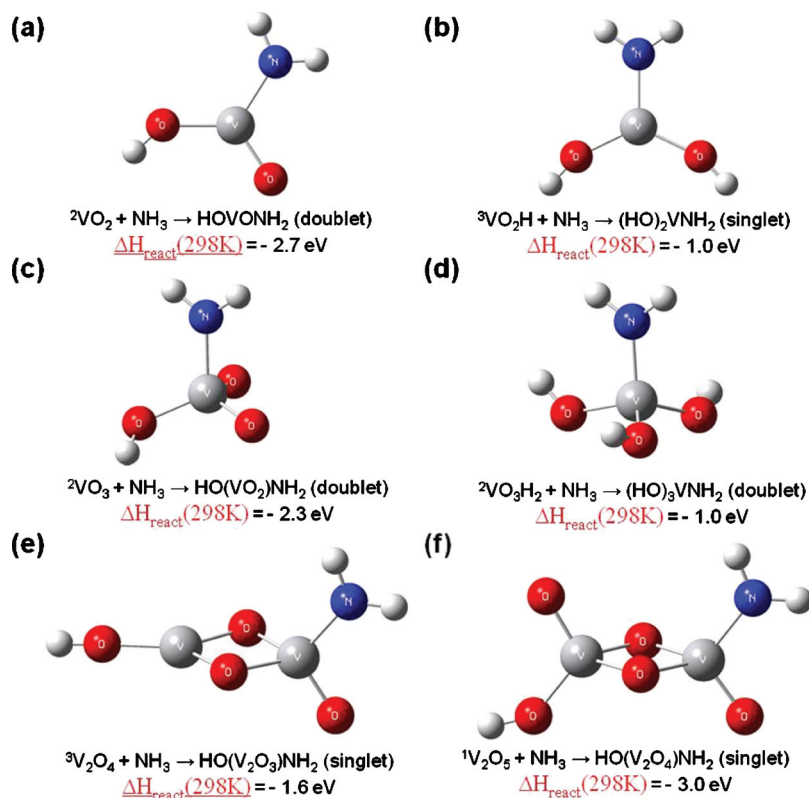
(a)

(b)

$^2VO_2 + NH_3 \rightarrow HOVONH_2$ (doublet)
$\Delta H_{react}(298K) = -2.7$ eV

$^3VO_2H + NH_3 \rightarrow (HO)_2VNH_2$ (singlet)
$\Delta H_{react}(298K) = -1.0$ eV

(c)

(d)

$^2VO_3 + NH_3 \rightarrow HO(VO_2)NH_2$ (doublet)
$\Delta H_{react}(298K) = -2.3$ eV

$^2VO_3H_2 + NH_3 \rightarrow (HO)_3VNH_2$ (doublet)
$\Delta H_{react}(298K) = -1.0$ eV

(e)

(f)

$^3V_2O_4 + NH_3 \rightarrow HO(V_2O_3)NH_2$ (singlet)
$\Delta H_{react}(298K) = -1.6$ eV

$^1V_2O_5 + NH_3 \rightarrow HO(V_2O_4)NH_2$ (singlet)
$\Delta H_{react}(298K) = -3.0$ eV

FIG. 4. DFT results showing the most stable structures for reaction products (a) VO_2NH_3, (b) $HVO_2(NH_3)$, (c) VO_3NH_3, (d) $H_2VO_3H_2(NH_3)$, (e) $V_2O_4NH_3$, and (f) $V_2O_5NH_3$. DFT calculations for Ta_mO_n clusters reveal similar structures.

B. Structure and reaction mechanism for neutral $M_mO_n+NH_3$

1. Experimental results

Figure 1(c) displays the mass spectrum of reactants and products for the reaction of V_mO_n clusters with NH_3, generated by 26.5 eV single photon ionization. V_mO_n clusters are much more reactive with NH_3 than they are with NO_x. Many association products are observed when NH_3 is added to the fast flow reactor. Products $VONH_3$, $VO_2(NH_3)_{1,2}$, $VO_2(NH_3)H$, $VO_3(NH_3)H_2$, $V_2O_4NH_3$, $V_2O_5NH_3$, $V_2O_5(NH_3)H$, $V_2O_6(NH_3)H_2$, etc., are readily detected. They are generated from association reactions,

$$M_mO_nH_{0,1,2} + NH_3 \rightarrow M_mO_nH_{0,1,2}NH_3, \qquad (3)$$

and are stabilized by collisions with third bodies (Table II). Mostly oxygen-stable and oxygen-rich clusters are involved in these association reactions. An additional hydrogen(s) is observed in some of the products [e.g., $VO_3(NH_3)H_2$, $V_2O_5(NH_3)H$, etc.]. These clusters most likely arise from the association of ammonia with corresponding $V_mO_nH_x$ clusters [e.g., VO_3H_2, V_2O_5H, etc., see Fig. 1(a)]. Since the features of association product $V_mO_nH_x(NH_3)$ clusters [Fig. 1(c)] are similar to those for $V_mO_nH_x$ clusters in the absence of NH_3 in the reaction cell [Fig. 1(a)], they can be assigned as arising directly from the original $V_mO_nH_x$ species in the beam. The additional hydrogen atoms could also come from the dissociation of NH_3 molecules and attachment of xH to the corresponding clusters, for example in the reaction $VO_3+NH_3 \rightarrow VO_3NH_3$, and then $VO_3NH_3+2H \rightarrow VO_3(NH_3)H_2$.

Ta_mO_n clusters behave in a similar fashion to V_mO_n clusters for the reactions $Ta_mO_n+NH_3$. Figure 2(a) displays the

Ta_mO_n cluster distribution (lower spectrum) and Fig. 2(c) displays reaction products (upper spectrum) when NH_3 is added to the reaction cell. Association products are observed as listed in Table II. These products are also generated from association reactions [Eq. (3)]. Mostly oxygen-stable and oxygen-rich clusters are involved in the association products. Similar to $V_mO_n(NH_3)_yH_x$ clusters, observed $Ta_mO_n(NH_3)_yH_x$ clusters arise mostly from association of ammonia with a corresponding $Ta_mO_nH_x$ cluster [e.g., TaO_3H_2, Ta_2O_5H, etc., see Fig. 2(a)].

2. Theoretical results

Figure 4 displays the results of DFT calculations for the lowest energy structures of the reaction products for $V_mO_n(H)_{0,1,2}+NH_3$. In each case, the addition of NH_3 to any cluster is followed by a hydrogen transfer to form $H(V_mO_n)$ and a V—NH_2 moiety in intermediate structures. On the basis of our calculations, the association energies for VO_3/TaO_3+NH_3 to form HVO_3NH_2 and HTO_3NH_2 are 2.0 and 2.1 eV, respectively. Hydrogen transfers from NH_3 to VO_3 and TaO_3 are a thermodynamically available without barriers. As shown in Fig. 5, several transition states are involved in the hydrogen transfer from NH_3 to the O atom of V_2O_5 for formation of the lowest energy structure for $HO(V_2O_4)NH_2$. The overall reaction is barrierless. Such structures and mechanisms are consistent with those proposed by many authors,[8,14,17,18,29] based on condensed phase experiments and DFT calculations. Further dissociation of the NH_2 moiety is found to be less favorable. The NH_2 moiety preferentially binds to the vanadium atom via a V—N bond. Comparing Figs. 1(c) and 2(c), one notes that the association products are similar for both V_mO_n and Ta_mO_n
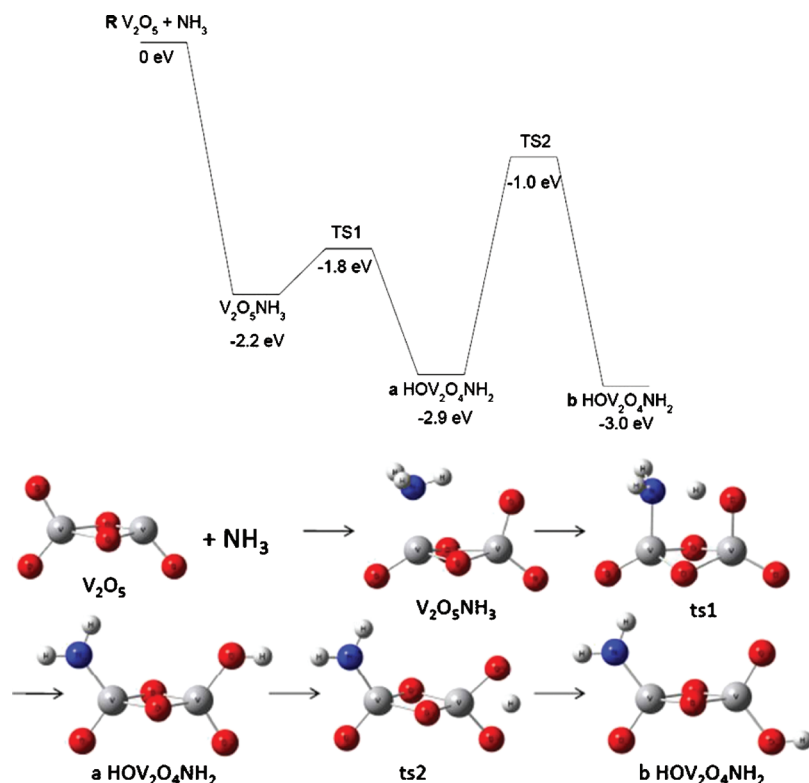
FIG. 5. DFT calculated potential energy surface for the $V_2O_5 + NH_3$ reaction. Structures are the optimized geometries of the reaction intermediates and transition states. Relative energies are in eV.

clusters reacting with NH_3, indicating that association energies and structures for V_mO_n/NH_3 and Ta_mO_n/NH_3 products should be similar. On the basis of our DFT calculations, association enthalpies ($\Delta H_{react}(298 \text{ K})$) for $NH_3 + Ta_mO_n$ clusters fall within $\pm 15\%$ of those calculated for $NH_3 + V_mO_n$ clusters.

Anstrom *et al.*[26] calculate NH_3 adsorption forming a stabilized NH_4^+ unit which corresponds to the ammonia molecule interaction with a VOH site. These theoretical results find an adsorption energy between 7 and 30 kcal/mol for molecular NH_3 on V_2O_5 (0 0 1).[26,27] In our experiments, we find that vanadium oxide clusters can readily adsorb H atoms and such clusters are present in the molecular beam as $V_mO_nH_x$ (VO_2H, VO_3H_2, V_2O_5H, and $V_2O_6H_2$), especially for oxygen-rich clusters. The presented calculated structures displayed in Fig. 4 clearly show a preference for a NH_2 species (and an H transfer to O) rather than an NH_4 species for the absorbed ammonia on both $V_mO_nH_{0,1,2}$ and $Ta_mO_nH_{0,1,2}$ cluster series. Separate and specific calculations (e.g., with periodic boundary conditions) for ionic species are not applied because a consistent set of calculated energies, structures, and chemistries for a true comparison of systems behavior is required.

Experimentally, the abundance of products in the reaction $M_mO_n + NH_3$ suggests that the interaction of M_mO_n with ammonia is much stronger than the interaction of M_mO_n with NO. These experimental results imply that in the condensed phase, the SCR proceeds according to an Eley–Rideal type mechanism in which ammonia is adsorbed on the catalyst in the first step. DFT calculations suggest that the association energy for NH_3 and M_mO_n is in general larger than the association energy for NO and M_mO_n. Therefore, in a competitive environment, ammonia will be preferentially adsorbed

on a vanadium oxide surface as the first step, rather than NO in the SCR process. DFT calculations also imply that ammonia adsorbs on V_mO_n clusters and then dissociates to form an NH_2 moiety via H transfer from NH_3 to an O atom of V_mO_n. The formation of an NH_2 moiety will favor NO adsorption through N—N bond formation, as is required for final product N_2 formation. The addition of an $NO : NH_3$ (9:1) mixture is examined in the next section.

C. Structure and reaction mechanism for neutral $M_mO_n + NO : NH_3$ (9:1)

1. Experimental results

To study the reactions of M_mO_n clusters in the presence of NO and NH_3, a mixture of $NO : NH_3$ is added to the fast flow reaction cell with a ratio of concentration 9:1. Figure 1(d) displays the mass spectrum of reactants and products for the reaction of V_mO_n clusters with $NO : NH_3$, generated by 26.5 eV single photon ionization. When compared to Fig. 1(c), one finds that the two mass spectra are nearly identical. The V_mO_n cluster system behaves as if only NH_3 were present in the reactor; in other words, no combined $V_mO_n + NH_3/NO$ adducts are detected in the mass spectrum.

Figure 2(d) displays the mass spectrum of Ta_mO_n clusters and their products when the same 9:1 ratio of $NO : NH_3$ is added to the reactor. One can observe that a new cluster series is found that contains the adduct of both an NO and an NH_3 molecule to form the products $TaO_2(NH_3)NO$, $TaO_3(NH_3)NO$, $Ta_2O_5(NH_3)NO$, and $Ta_2O_6(NH_3)NO$ compared to Fig. 2(c). The general reaction is
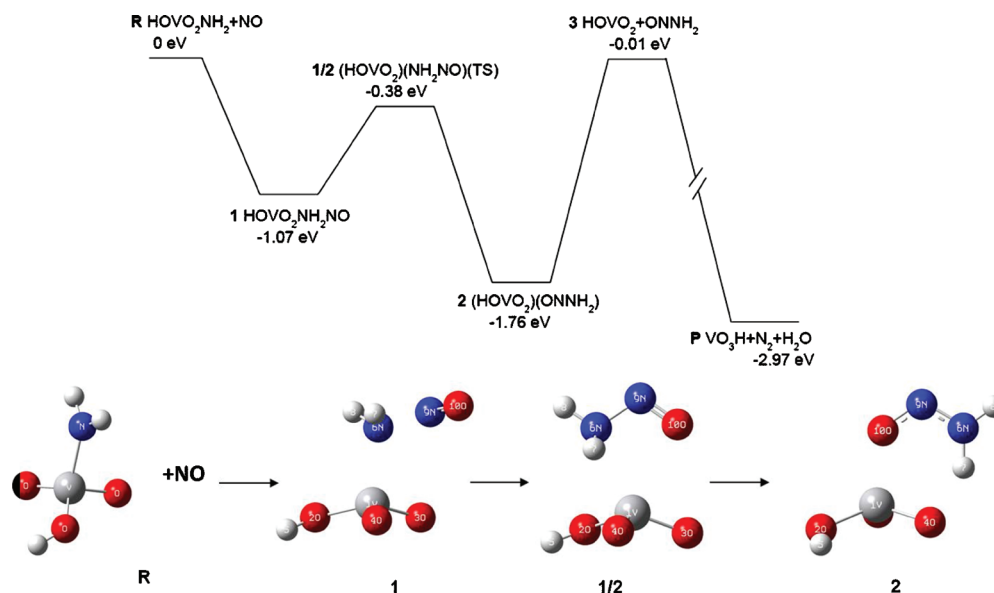
FIG. 6. DFT calculated potential energy surface for the $VO_3+NO:NH_3$ reaction. Structures are the optimized geometries of the reaction intermediates and transition states. Relative energies are in eV.

$$Ta_mO_n + NO:NH_3(9:1) \rightarrow Ta_mO_n(NH_3)NO. \qquad (4)$$

These reactions are also explored with different $NO:NH_3$ ratios beginning at 1:1. The low concentration of NO proved to be insufficient to compete with the strong reactivity of NH_3, and $Ta_mO_n(NH_3)NO$ signals in the mass spectra are very weak. Signal intensities of the $Ta_mO_n(NH_3)NO$ products are relatively stronger at 9:1 ratio of $NO:NH_3$.

Based on different behavior in the experiments for the vanadium and tantalum cluster series, one might conclude from these experimental results that tantalum oxide clusters are more active with the gas mixture and might be a better catalyst for the SCR of NO using ammonia. In order to explore and elucidate this interpretation, the reaction mechanism and potential energy surface for the $MO_3+NO:NH_3$ reaction system is explored via the DFT methods described above.

2. Theoretical results

Oxygen-rich V_mO_n and Ta_mO_n clusters are more reactive with NO than oxygen deficient and stable clusters; for example, most of the association products M_mO_nNO (VO_3NO, TaO_3NO, TaO_4NO, Ta_2O_6NO, Ta_3O_8NO, etc.) are generated for oxygen-rich clusters. The mixed association product $TaO_3(NH_3)NO$ is observed in the reaction of Ta_mO_n $+NH_3/NO$. In our previous studies,[39,40,43] we found that VO_3 can be considered as an active center for larger clusters, represented as structures $VO_3(V_2O_5)_n$. Therefore, we select the relatively small clusters VO_3 and TaO_3 to model the reaction systems of V_mO_n/Ta_mO_n and NH_3/NO. To calculate the structures, mechanisms, and surfaces for coadsorption of NO and ammonia on both V_mO_n and Ta_mO_n clusters, we start from the lowest energy structure for one ammonia molecule on an MO_3 cluster and add an NO molecule to the system. The lowest energy structures calculated favor the placement of NO and NH_3 in the same region of the cluster.

Based on the calculation results for the reaction VO_3 $+NO:NH_3$ (9:1), the reaction begins with the optimized structure of VO_3+NH_3 (**R** $HOVO_2NH_2$) as shown in Fig. 6. The reaction starts by introducing an NO molecule to form intermediate **1** in which the N from the NH_2 radical and the N from the NO are weakly bound. Via transition structure **1/2**, a lowest energy intermediate **2** with two moieties, $ONNH_2$ and $HOVO_2$, is formed. The two moieties can then separate and proceed to product **3** consisting of two separate molecules. A free $ONNH_2$ molecule now is produced. Final production of N_2+H_2O from $ONNH_3$ involves a complex mechanism that has no barrier with respect to the final product formation reaction $ONNH_2 \rightarrow N_2+H_2O$, as discussed in the literature.[1,58,59] Our calculations show that vanadium oxide clusters form a weakly bound intermediate **2** that can separate into **3** $HOVO_2+ONNH_2$ and can then follow the reaction pathway to form products **P** N_2+H_2O in an overall barrierless reaction. We suggest that these latter steps are the reason that no intermediate product species, involving a V_mO_n cluster with both NO and ammonia molecules, are observed in the mass spectrum [Fig. 1(d)]. Thus, V_mO_n clusters can react with NO and NH_3 to generate N_2 and H_2O.

The above described mechanistic steps represent the behavior of a good catalyst that does not form stable intermediates, but forms weakly bound complexes available for further reaction. As with the condensed phase system, the product $HOVO_2$ could further react with O_2 to complete a catalytic cycle under certain conditions through following reactions (5) and (6):

$$VO_3 + NO + NH_3 \rightarrow HOVO_2 + N_2 + H_2O, \qquad (5)$$

$$2HOVO_2 + 1/2O_2 \rightarrow H_2O + 2VO_3. \qquad (6)$$

The same calculations for tantalum oxide clusters are also conducted. The reaction between NO and ammonia supported by Ta_mO_n clusters starts with the optimized structure
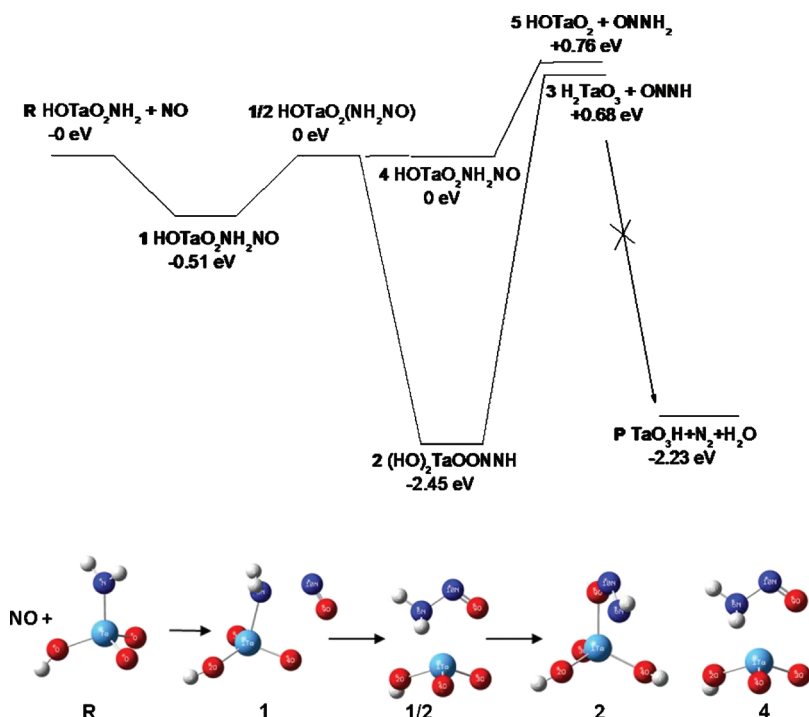
FIG. 7. DFT calculated potential energy surface for $TaO_3 + NO : NH_3$ reaction. Structures are the optimized geometries of the reaction intermediates and transition states. Relative energies are in eV.

of the model system $TaO_3 + NH_3$ (**R** $HOTaO_2NH_2$) as shown in Fig. 7. The reaction proceeds in a very similar way to that for vanadium oxide clusters up to transition structure **1/2**: adding an NO molecule forms intermediate **1** in which the N of the NH_2 radical and the N of the NO radical are weakly bound. The difference between the VO_3 and TaO_3 reactions occurs via transition structure **1/2**, leading to a very stable lowest energy intermediate **2** ($(HO)_2TaOONNH$) for the Ta species. Here, the vanadium oxide intermediate **2** (Fig. 6) partitions into two separate radicals whereas the tantalum oxide intermediate **2** (Fig. 7) forms a stable complex via hydrogen transfer. Generation of product **3** H_2TaO_3 $+ONNH$ is thermodynamically and kinetically unavailable for the tantalum oxide reaction. The calculation results suggest that the reaction should not proceed to form the final products $N_2 + H_2O$. This formation of a stable intermediate for tantalum oxide clusters implies that tantalum oxide clusters should not be a good catalyst for the SCR of NO with ammonia in the condensed phase. The formation of ionic intermediate species of the form $(NH_4^+)(M_mO_n^-)$ is a higher energy pathway than the formation of the radical like species $(HOM_mO_{n-1})(NH_2)(NO)$.

The potential energy surface for the reaction $HOVO_2NH_2 + NO$ (Fig. 6) shows that the reaction has two intermediates $HOVO_2NH_2NO$ (**1**) and $(HOVO_2)(ONNH_2)$ (**2**). The lower energy intermediate (**2**) can dissociate into $HOVO_2 + ONNH_2$ (**3**) without an overall barrier. Intermediate **3** can in turn dissociate into products (**P**) $VO_3H + N_2$ $+ H_2O$. This reaction pathway is consistent with the observed mass spectral data for $V_mO_n + NH_3 + NO$ reactions and the mechanism suggested explains the observations. Next consider the potential energy surface for the comparable reaction with TaO_3 (Fig. 7). A stable local minimum energy intermediate structure, $HOTaO_2NH_2NO$ (**1**), is again found but this is connected through a transition state to a lower energy in-

termediate $(HO)_2TaOONNH$ (**2**) and a higher energy intermediate $HOTaO_2NH_2NO$ (**4**). Intermediates **2** and **4** here connect to intermediates **3** and **5**, respectively, both of which are higher in energy than the reactants. Thus, the reaction stops at $(HO)_2TaOONNH$ (**2**) rather than going on to products $TaO_3H + N_2 + H_2O$. For TaO_3, a structure similar to the VO_3 reaction $(HOVO_2)(ONNH_2)$ (Fig. 6, **2**), cannot be found for the potential surface for $HOTaO_2NH_2 + NO$ because a second H atom transfers to the TaO_3 moiety to form the lowest energy intermediate $(HO)_2TaOONNH$ (Fig. 7, **2**). Therefore, the reaction $HOTaO_2NH_2 + NO$ cannot go through the same reaction pathway as $HOVO_2NH_2 + NO$ and the reaction to $N_2 + H_2O$ does not proceed.

What we have discussed shows that the DFT reaction potential energy surface and structure calculations do indeed indicate that the V_mO_n cluster system is the reactive one and does model the condensed phase vanadium oxide promoted reaction as stated in the Introduction. Also, based on the DFT results, the Ta_mO_n system would not be a good catalyst since the intermediates do not readily yield products due to dynamic effects, i.e., reaction barriers. The experimental observations of cluster reaction intermediates and products are consistent with the calculated reaction behavior of the clusters and the condensed phase behavior of the modeled V_mO_n catalyst. Experiments were also conducted using neutral Nb_mO_n clusters and the results matched those obtained for V_mO_n clusters.

V. CONCLUSIONS

In the present work, the reactivity of neutral vanadium and tantalum oxide clusters toward NO, NH_3, and an NO/NH_3 mixture is explored experimentally and theoretically. Our motivation is to understand possible molecular level mechanisms for the SCR of NO by NH_3 in condensed

phase catalytic reactions. We find that oxygen-rich V_mO_n and Ta_mO_n clusters are more reactive toward NO than oxygen deficient and stable clusters. If ammonia is added to the fast flow reactor in place of NO_x, both V_mO_n and Ta_mO_n clusters behave in a similar manner and form many association products identified in the observed mass spectra. If a gas mixture of $NO:NH_3$ (9:1) is added to the reactor, the two cluster systems behave differently. The mass spectrum of V_mO_n clusters reveals no new products for the coadsorption of NO and NH_3. Ta_mO_n clusters, on the other hand, form a new cluster series that does involve coadsorption of NO and NH_3. DFT calculations suggest that Ta_mO_n clusters form stable cluster complexes based on the coadsorption of NO and ammonia and that these products are thermodynamically and kinetically stable. V_mO_n clusters form weakly bound complexes that can follow the reaction path toward end products N_2+H_2O. Thus, cluster intermediates involving $NO+NH_3$ are not observed in the mass spectrum. Overall, our results suggest that vanadium oxide should make a better catalyst for the SCR of NO with NH_3 than tantalum oxide. Both our theoretical and experimental results support a radical reaction mechanism in which NH_2 is the important moiety for the V_mO_n based catalytic conversion of NO and NH_3 to N_2 and H_2O. A complete catalytic cycle is generated if the hydrogenated oxygen-rich site reacts with ambient oxygen to form water and the original catalyst.

[1] S. Soyer, A. Uzun, S. Senkan, and I. Onal, Catal. Today **118**, 268 (2006).
[2] M. L. Ferreira and M. Volpe, J. Mol. Catal. Chem. **164**, 281 (2000).
[3] L. Pinaeva, A. P. Suknev, A. A. Budneva, E. A. Paukshtis, and B. S. Balzhinimaev, J. Mol. Catal. **112**, 115 (1996).
[4] G. C. Bond and S. Flamertz, Appl. Catal. **71**, 1 (1991).
[5] G. T. Went, L. J. Leu, S. J. Lombardo, and A. T. Bell, J. Phys. Chem. **96**, 2235 (1992).
[6] M. Inomata, A. Miyamoto, and Y. Murakami, J. Catal. **62**, 140 (1980).
[7] M. Inomata, A. Miyamoto, and Y. Murakami, J. Phys. Chem. **85**, 2372 (1981).
[8] F. J. J. G. Janssen, F. M. G. van den Kerkhof, H. Bosch, and J. R. H. Ross, J. Phys. Chem. **91**, 5921 (1987).
[9] F. J. J. G. Janssen and F. M. G. van den Kerkhof, J. Phys. Chem. **91**, 6633 (1987).
[10] N.-Y. Topsøe, J. Catal. **128**, 499 (1991).
[11] N.-Y. Topsøe, H. Topsøe, and J. A. Dumesic, J. Catal. **151**, 226 (1995).
[12] N.-Y. Topsøe, H. Topsøe, and J. A. Dumesic, J. Catal. **151**, 241 (1995).
[13] M. G. Gasior, J. Haber, T. Machej, and T. Czeppe, J. Mol. Catal. **43**, 359 (1988).
[14] U. S. Ozkan, Y. Cai, and M. W. Kumthekar, J. Catal. **149**, 390 (1994).
[15] G. Ramis, L. Yi, G. Busca, M. Turco, E. Kotur, and R. J. Willey, J. Catal. **157**, 523 (1995).
[16] G. Ramis, L. Yi, and G. Busca, Catal. Today **28**, 373 (1996).
[17] G. Busca, L. Lietti, G. Ramis, and F. Berti, Appl. Catal., B **18**, 1 (1998).
[18] M. Calatayud, B. Mguig, and C. Minot, Surf. Sci. Rep. **55**, 169 (2004).
[19] G. Deo and I. E. Wachs, J. Catal. **146**, 323 (1994).
[20] H. Schneider, S. Tschudin, M. Schneider, A. Wokaun, and A. Baiker, J. Catal. **147**, 5 (1994).
[21] M. A. Centeno, I. Carrizosa, and J. A. Odriozola, Appl. Catal., B **19**, 67 (1998).
[22] M. Farber and S. P. Harris, J. Phys. Chem. **88**, 680 (1984).
[23] T. Komatsu, M. Nunokawa, S. Moon, T. Takahara, D. Namba, and T. Yashima, J. Catal. **148**, 427 (1994).
[24] F. Gilardoni, J. Weber, and A. Baiker, Int. J. Quantum Chem. **61**, 683 (1997).
[25] F. Gilardoni, J. Weber, and A. Baiker, J. Phys. Chem. A **101**, 6069 (1997).
[26] M. Anstrom, N.-Y. Topsøe, and J. A. Dumesic, Catal. Lett. **78**, 281 (2002).
[27] M. Anstrom, N.-Y. Topsøe, and J. A. Dumesic, J. Catal. **213**, 115 (2003).
[28] X. Yin, H. Han, and A. Miyamoto, Phys. Chem. Chem. Phys. **2**, 4243 (2000).
[29] K. Jug, T. Homann, and T. Bredow, J. Phys. Chem. A **108**, 2966 (2004).
[30] N. U. Zhanpeisov, S. Higashimoto, and M. Anpo, Int. J. Quantum Chem. **84**, 677 (2001).
[31] N. A. Kachurovskaya, E. P. Mikheeva, and G. M. Zhidomirov, J. Mol. Catal. A: Chem. **178**, 191 (2002).
[32] E. P. Mikheeva, N. A. Kachurovskaya, and G. M. Zhidomirov, Kinet. Catal. **43**, 223 (2002).
[33] Y. Izumi, F. Kiyotaki, H. Yoshitake, K. Aika, T. Sugihara, T. Tatsumi, Y. Tanizawa, T. Shido, and Y. Iwasawa, Chem. Commun. (Cambridge) **2002**, 2402.
[34] T. Homann, T. Bredow, and K. Jug, Surf. Sci. **515**, 205 (2002).
[35] S. Heinbuch, F. Dong, J. J. Rocca, and E. R. Bernstein, J. Opt. Soc. Am. A **25**, B85 (2008).
[36] S. Heinbuch, F. Dong, J. J. Rocca, and E. R. Bernstein, J. Chem. Phys. **126**, 244301 (2007).
[37] S. Heinbuch, F. Dong, J. J. Rocca, and E. R. Bernstein, J. Chem. Phys. **125**, 154316 (2006).
[38] F. Dong, S. Heinbuch, X. Yan, J. J. Rocca, and E. R. Bernstein, J. Phys. Chem. A **113**, 3029 (2009).
[39] F. Dong, S. Heinbuch, Y. Xie, J. J. Rocca, Z. Wang, K. Deng, S. He, and E. R. Bernstein, J. Am. Chem. Soc. **131**, 1057 (2009).
[40] F. Dong, S. Heinbuch, Y. Xie, J. J. Rocca, Z. Wang, K. Deng, S. He, and E. R. Bernstein, J. Am. Chem. Soc. **130**, 1932 (2008).
[41] F. Dong, S. Heinbuch, J. J. Rocca, and E. R. Bernstein, J. Chem. Phys. **124**, 224319 (2006).
[42] F. Dong, S. Heinbuch, J. J. Rocca, and E. R. Bernstein, J. Chem. Phys. **125**, 154317 (2006).
[43] F. Dong, S. Heinbuch, J. J. Rocca, and E. R. Bernstein, J. Chem. Phys. **125**, 164318 (2006).
[44] S. Heinbuch, M. Grisham, D. Martz, and J. J. Rocca, Opt. Express **13**, 4050 (2005).
[45] S. Heinbuch, M. Grisham, D. Martz, F. Dong, E. R. Bernstein, and J. J. Rocca, Proc. SPIE **5919**, 591907 (2005).
[46] M. J. Frisch, G. W. Trucks, H. B. Schlegel et al., GAUSSIAN03, Revision B.04, Gaussian, Inc., Pittsburgh, PA, 2003.
[47] C. Peng and H. B. Schlegel, Isr. J. Chem. **33**, 449 (1994).
[48] C. Peng, P. Y. Ayala, H. B. Schlegel, and M. J. Frisch, J. Comput. Chem. **17**, 49 (1996).
[49] C. Gonzalez and H. B. Schlegel, J. Chem. Phys. **90**, 2154 (1989); J. Phys. Chem. **94**, 5523 (1990).
[50] A. D. Becke, Phys. Rev. A **38**, 3098 (1988); J. Chem. Phys. **98**, 5648 (1993); C. Lee, W. Yang, and R. G. Parr, Phys. Rev. B **37**, 785 (1988).
[51] A. Schafer, C. Huber, and R. J. Ahlrichs, Chem. Phys. **100**, 5829 (1994).
[52] L. E. Roy, P. J. Hay, and R. L. Martin, J. Chem. Theory Comput. **4**, 1029 (2008).
[53] S. F. Boys and F. Bernardi, Mol. Phys. **19**, 553 (1970); S. Simon, M. Duran, and J. J. Dannenberg, J. Chem. Phys. **105**, 11024 (1996).
[54] (a) K. P. Huber and G. Herzberg, Molecular Spectra and Molecular Structure Constants of Diatomic Molecules (VanNostrand, New York, 1979); (b) D. F. McMillen and D. M. Golden, Annu. Rev. Phys. Chem. **33**, 493 (1982); (c) J. B. Pedley and E. M. Marshall, J. Phys. Chem. Ref. Data **12**, 967 (1983); (d) J. Xu, M. T. Rodgers, J. B. Griffin, and P. B. Armentrout, J. Chem. Phys. **108**, 9339 (1998); (e) C. S. Hinton, F. X. Li, and P. B. Armentrout, Int. J. Mass. Spectrom. **280**, 226 (2009).
[55] M. Calatayud, J. Andres, and A. Beltran, J. Phys. Chem. A **105**, 9760 (2001).
[56] E. Jakubikova, A. K. Rappé, and E. R. Bernstein, J. Phys. Chem. A **111**, 12938 (2007); E. Jakubikova, Ph.D. dissertation, Colorado State University, 2007.
[57] (a) S. Feyel, D. Schroder, and H. Schwarz, J. Phys. Chem. A **110**, 2647 (2006); (b) R. C. Bell, K. A. Zemski, K. P. Kerns, H. T. Denkg, and A. W. Castleman, J. Phys. Chem. A **102**, 1733 (1998).
[58] X. Duan and M. Page, J. Mol. Struct. **333**, 233 (1995).
[59] S. P. Walch, J. Chem. Phys. **99**, 5295 (1993).